



This discussion paper is/has been under review for the journal Atmospheric Chemistry and Physics (ACP). Please refer to the corresponding final paper in ACP if available.

CALIOP near-real-time backscatter products compared to EARLINET data

T. Grigas¹, M. Hervo^{1,*}, G. Gimmestad², H. Forrister^{2,**}, P. Schneider³,
J. Preißler¹, L. Tarrason³, and C. O'Dowd¹

¹School of Physics and Centre for Climate and Air Pollution Studies, Ryan Institute, National University of Ireland Galway, Galway, Ireland

²Electro-Optical Systems Laboratory, Georgia Tech Research Institute, Georgia Institute of Technology, 225 North Avenue, Atlanta, Georgia 30332, USA

³NILU – Norwegian Institute for Air Research, P.O. Box 100, 2027 Kjeller, Norway

* now at: Federal Office of Meteorology and Climatology, MeteoSwiss, Payerne 1530, Switzerland

** now at: School of Earth and Atmospheric Sciences, Georgia Institute of Technology, 225 North Avenue, Atlanta, Georgia 30332, USA

Received: 17 December 2014 – Accepted: 9 February 2015 – Published: 4 March 2015

Correspondence to: T. Grigas (tomas.grigas@nuigalway.ie)

Published by Copernicus Publications on behalf of the European Geosciences Union.

Title Page

Abstract

Introduction

Conclusions

References

Tables

Figures



Back

Close

Full Screen / Esc

Printer-friendly Version

Interactive Discussion



Abstract

The expedited near-real-time Level 1.5 Cloud–Aerosol Lidar (Light Detection and Ranging) with Orthogonal Polarization (CALIOP) products were evaluated against data from the ground-based European Aerosol Research Lidar Network (EARLINET). Over a period of three years, lidar data from 48 CALIOP overpasses with ground tracks within a 100 km distance from an operating EARLINET station were deemed suitable for analysis and they included a valid aerosol classification type (e.g. dust, polluted dust, clean marine, clean continental, polluted continental, mixed and/or smoke/biomass burning). For the complete dataset comprising both PBL and FT data, the correlation coefficient was 0.86, and when separated into separate layers, the PBL and FT correlation coefficients were 0.6 and 0.85 respectively. The presence of FT layers with high attenuated backscatter led to poor agreement in PBL backscatter profiles between the CALIOP and EARLINET measurements and prompted a further analysis filtering out such cases. However, the correlation coefficient value for the complete dataset decreased marginally from 0.86 to 0.84 while the PBL coefficient increased from 0.6 up to 0.65 and the FT coefficient also decreased from 0.85 to 0.79. For specific aerosol types, the correlation coefficient between CALIOP backscatter profiles and ground-based lidar data ranged from 0.37 for polluted continental aerosol in the planetary boundary layer (PBL) to 0.57 for dust in the free troposphere (FT). The results suggest different levels of agreement based on the location of the dominant aerosol layer and the aerosol type.

1 Introduction

Aerosols have an impact on the global radiative budget directly via scattering and absorbing incoming solar radiation, and indirectly, via the modification of cloud microphysical properties that lead to changes in cloud radiative properties along with cloud lifetimes (Haywood et al., 2003; Yu et al., 2006). Lidar is a very useful technique for

ACPD

15, 6041–6075, 2015

CALIOP
near-real-time
backscatter products

T. Grigas et al.

Title Page

Abstract

Introduction

Conclusions

References

Tables

Figures

◀

▶

◀

▶

Back

Close

Full Screen / Esc

Printer-friendly Version

Interactive Discussion



CALIOP
near-real-time
backscatter products

T. Grigas et al.

Title Page

Abstract

Introduction

Conclusions

References

Tables

Figures



Back

Close

Full Screen / Esc

Printer-friendly Version

Interactive Discussion



characterising the vertical dispersion of aerosol plumes through examination of the backscatter signal and aerosol properties such as shape, from the polarization signal, that can elucidate particle composition, in particular, for Saharan dust or volcanic ash plumes (Groß et al., 2010; Papayannis et al., 2002). Several research programmes in Europe performed routine long-term observations of the optical properties of different aerosol types (Giannakaki et al., 2009; Mattis et al., 2004, 2008); however, such studies were typically limited to single geographical locations. In order to study aerosol transport on a larger spatial scale, lidar networks are deployed (Pappalardo et al., 2009b), in conjunction with space borne platforms. In 2000, EARLINET was established to provide a comprehensive statistically representative data set of the aerosol vertical distribution (Böckmann et al., 2004). At present, 28 European stations contribute to this network (Sawamura et al., 2012). Global coverage may be achieved by using satellite-based lidar systems and striving towards such an aim, the National Aeronautics and Space Administration (NASA), in collaboration with the French space agency Centre National d'Etudes Spatiales (CNES), developed a satellite-based lidar system called CALIOP, which is on board the CALIPSO satellite platform (Omar et al., 2009). CALIOP performs measurements simultaneously at wavelengths of 532 and 1064 nm. The CALIPSO satellite was launched into orbit in April 2006 and is part of the A-Train constellation of scientific satellites dedicated to observations of the atmosphere (Stephens et al., 2002). It follows a sun-synchronous polar orbit of 705 km altitude and has a 16 day repeat cycle.

The EARLINET community has performed several comparisons with CALIOP data since its launch in April 2006 (Mattis et al., 2007; Pappalardo et al., 2010) using CALIOP overpasses with ground tracks within 100 km from EARLINET stations. Several studies inter-comparing CALIOP Level 1 and Level 2 data with the ground-based measurements were performed in recent years (Mamouri et al., 2009; Molero and Pujadas, 2008; Pappalardo et al., 2009a, 2010). Pappalardo et al. (2010) found good agreement between the 532 nm CALIOP Level 1 attenuated backscatter and EARLINET measurements with a relative mean difference of 4.6 % and a relative SD of

CALIOP
near-real-time
backscatter products

T. Grigas et al.

Title Page

Abstract

Introduction

Conclusions

References

Tables

Figures



Back

Close

Full Screen / Esc

Printer-friendly Version

Interactive Discussion



50%. The attenuated backscatter was used only from those EARLINET stations that provided independent extinction measurements. The correlation coefficient as a function of the CALIOP ground track offset distances was assessed as well. The correlation coefficient $R = 0.9$ was found for distances smaller than 100 km, while it decreased rapidly with larger distances. The mean bias between the CALIOP Level 1 and EARLINET Athens station's measurements as assessed by (Mamouri et al., 2009) for daytime measurements was 22 %, and for night-time measurements, 8 %. Mona et al. (2009) found a mean difference of (-2 ± 12) % between data from the EARLINET station in Potenza and CALIOP Level 1 measurements within the 3–8 km altitude range, while the mean difference of the measurements within the PBL was equal to (-24 ± 20) %. The influence of the presence of cirrus clouds on the measurements was assessed in a study by Mamouri et al. (2009). The mean biases without cirrus clouds were -26 ± 22 % for 5 km horizontal resolution and -14 ± 15 % for 20 km; the biases were higher in cirrus cases with -104 ± 129 % for 5 km horizontal resolution and -85 ± 93 % for 20 km.

Assimilation of the CALIOP Level 1B data product into atmospheric models has been carried out successfully in the past using an ensemble Kalman filter (Sekiyama et al., 2010). However, processed CALIOP Level 1B and Level 2 data products are generally only available several days after acquisition at the earliest, thus severely limiting their use for operational data assimilation. An expedited CALIOP Level 1.5 near-real-time (NRT) product, usually provided between 6 and 30 h after downlink, has been made available by NASA for purposes of operational forecasting since November 2010. This product is derived (Powell et al., 2013) by spatially averaging the Level 1 profiles and merging them with the Level 2 vertical feature mask product.

The European Centre for Medium-Range Weather Forecasts (ECMWF) is currently evaluating the potential use of an expedited CALIOP Level 1.5 data product (the total attenuated backscatter profile) for assimilation into their global forecasting model IFS-MOZART (A. Benedetti, ECMWF, personal communication, 2014) under the Monitoring Atmospheric Composition and Climate (MACC) project. A similar idea of us-

ing ground-based lidar measurements in the model assimilation was implemented in a study by Wang et al. (2013). They found that the root mean square error (RMSE) of PM_{10} concentrations declined by 54 % when the lidar measurements were used in the assimilation. This indicates the importance of evaluating the CALIOP Level 1.5 data by inter-comparing them with ground-based measurements. The inter-comparison of the 532 nm wavelength attenuated backscatter profiles between CALIOP and EARLINET reported here was performed for coincident daytime and night-time measurements.

2 Data and methodology

The CALIOP instrument directly measures the vertical profile of the total attenuated backscatter as seen from above the atmosphere, with a spatial resolution of 30 m vertically and 333 m horizontally (Winker et al., 2009). This Level 0 raw data is averaged both horizontally and vertically before it is downlinked to the NASA Langley Research Centre (LaRC) where the scientific data products of the various levels are produced (Level 1, Level 1.5, Level 2 and Level 3). The vertical resolution for this processing level varies from 30 m (−0.5 to 8.2 km) up to 300 m (30.1 to 40 km), while the horizontal resolution varies from 333 m (−0.5 to 8.2 km) up to 5 km (30.1 to 40 km) (Powell et al., 2013).

CALIOP has an automatic aerosol classification algorithm that uses altitude, location, surface type, volume depolarization ratio δ_v and integrated attenuated backscatter γ' at 532 nm to determine the aerosol type (Burton et al., 2013; Omar et al., 2009). The algorithm detects eight main aerosol types: clean air, clean marine, polluted dust, dust, polluted continental, clean continental, smoke/burning biomass and mixed aerosols. The Level 2 vertical feature mask provides information on cloud and aerosol layers as well as the type of aerosol in each identified layer.

The Level 1.5 product is derived by spatially averaging 60 individual Level 1 lidar profiles and merging them with the Level 2 vertical feature mask product. It has a spatial resolution of 20 km horizontally and 60 m vertically and it is restricted to the altitude

Title Page

Abstract

Introduction

Conclusions

References

Tables

Figures



Back

Close

Full Screen / Esc

Printer-friendly Version

Interactive Discussion



range -0.5 to 20 km (Powell et al., 2013). The main Level 1.5 parameters used in this work are latitude, longitude, profile UTC time, mean total attenuated backscatter profile at 532 nm, SD of the total attenuated backscatter for 532 nm, total attenuated backscatter uncertainty for 532 nm (CALIPSO Quality Statements, 2011, p. 02) L2 feature type, and lidar ratio, along with the Rayleigh extinction and backscatter cross sections for the molecular atmosphere at 532 nm.

The CALIOP uncertainties of the attenuated backscatter (CALIPSO Quality Statements, 2011) are calculated using the equation

$$\sigma_{\mu} = \frac{1}{N} \sqrt{\sum_{i=1}^N \sigma_i^2}, \quad (1)$$

where σ_i is the attenuated backscatter uncertainty at the range bin μ and N is the number of Level 1 profile range bins.

EARLINET was chosen as the reference network for this inter-comparison. At present, this network is one of the most sophisticated lidar networks in the world. The ground-based lidar measurements used in this study were acquired from the EARLINET portal www.EARLINET.org for the period from November 2010 to December 2012 as well as for several days in April and May 2010 during the Eyjafjallajökull volcano eruption. The aerosol backscatter coefficient profiles with uncertainties were provided in each of the EARLINET files. CALIOP-EARLINET inter-comparisons were only considered for coincident overpasses, defined as having a CALIOP ground track within a 100 km distance from the EARLINET station. The backscatter coefficients provided by EARLINET were converted into total attenuated backscatter values using the method described below.

The CALIOP instrument directly measures profiles of the total (molecular plus aerosol) attenuated backscatter as seen from space, and NASA provides them in the Level 1.5 data set. These profiles were chosen for the inter-comparison in order to assess CALIOP measurements. The EARLINET stations produce aerosol backscatter

CALIOP near-real-time backscatter products

T. Grigas et al.

[Title Page](#)[Abstract](#)[Introduction](#)[Conclusions](#)[References](#)[Tables](#)[Figures](#)[Back](#)[Close](#)[Full Screen / Esc](#)[Printer-friendly Version](#)[Interactive Discussion](#)

coefficients and so the two different backscatter coefficients cannot be inter-compared directly. For this reason, a method similar to that of Mona et al., (2009) was adopted for converting the EARLINET particulate backscatter coefficients into total attenuated backscatter values as observed from space, thus allowing for a valid inter-comparison of CALIOP and EARLINET measurements. The following equations were used to calculate EARLINET attenuated backscatter. The total attenuated backscatter $\beta_{\text{att}}(z)$ at altitude z is given by

$$\beta_{\text{att}}(z) = T^2(z)\beta_{\text{tot}}(z), \quad (2)$$

where $T^2(z)$ is the two-way transmittance from the lidar in space down to the altitude z , and β_{tot} is the total backscatter coefficient, defined as

$$\beta_{\text{tot}}(z) = \beta_{\text{par}}(z) + \beta_{\text{mol}}(z), \quad (3)$$

where β_{par} is the particulate (aerosol) backscatter coefficient, and β_{mol} is the molecular backscatter coefficient.

In order to calculate the total backscatter coefficient β_{tot} , the EARLINET particulate backscatter coefficient is used as β_{par} in Eq. (3) and the molecular backscatter coefficient β_{mol} is provided as a Level 1.5 data product. The two-way transmittance for a downward-looking lidar is calculated using the following equation:

$$T^2(z) = \exp \left[-2 \int_{\text{top}}^z \alpha(z') dz' \right], \quad (4)$$

where top is the highest altitude of the profile (nominally 20 km), and $\alpha(z)$ is the total extinction coefficient, which is the sum of the particle extinction coefficient α_{par} and the molecular extinction coefficient α_{mol} .

The particle extinction coefficient α_{par} is calculated according to

$$\alpha_{\text{par}} = S_a \beta_{\text{par}}, \quad (5)$$

**CALIOP
near-real-time
backscatter products**

T. Grigas et al.

Title Page

Abstract

Introduction

Conclusions

References

Tables

Figures



Back

Close

Full Screen / Esc

Printer-friendly Version

Interactive Discussion



where β_{par} is the EARLINET particle backscatter coefficient and S_a is the particulate extinction-to-backscatter ratio, (commonly known as the lidar ratio). The lidar ratios are provided by EARLINET stations only for a small fraction of the coincident measurements. The reason is that the lidar system needs to be equipped with a Raman channel for independent extinction profile measurements, and these measurements are available only during night-time because of low signal-to-noise ratio during daytime. Therefore, the lidar ratios used in this study corresponded to the aerosol types identified in the CALIOP Level 1.5 data set. The EARLINET extinction coefficients α_{par} were then calculated using Eq. (6).

After calculating the terms α_{mol} and α_{par} , the transmittance was derived using Eq. (5) and the EARLINET total attenuated backscatter profile was calculated using Eq. (2).

In order to reduce the noise in the CALIOP signal (especially during daytime), the five profiles of the CALIOP total attenuated backscatter closest to the EARLINET station were averaged and then compared to the total attenuated backscatter of the EARLINET station. All of our CALIOP data points therefore correspond to spatial averages 100 km in length along the ground tracks, centered at the points of closest approach to the EARLINET stations.

To enable direct comparisons, the altitude scales of the EARLINET lidar profiles were adjusted to be the same as that of CALIOP (above mean sea level) at 60 m vertical spacing. In this way we obtained pairs of values at each altitude, referred to here as “data points”, for each overpass.

In this work, the total attenuated backscatter for CALIOP ($\beta_{\text{att,CAL}}$) and EARLINET ($\beta_{\text{att,EARL}}$) are inter-compared. In order to quantify the agreement between CALIOP and EARLINET measurements, the correlation coefficient, the mean bias, and the factor of exceedance are used (Kristiansen et al., 2012). Their defining equations are provided below.

The correlation coefficient R is defined in the usual way as

$$R = \frac{\sum_{i=1}^N (\beta_{\text{att.CAL}_i} - \overline{\beta_{\text{att.CAL}}}) (\beta_{\text{att.EAR}_i} - \overline{\beta_{\text{att.EAR}}})}{\sqrt{\sum_{i=1}^N (\beta_{\text{att.CAL}_i} - \overline{\beta_{\text{att.CAL}}})^2} \sqrt{\sum_{i=1}^N (\beta_{\text{att.EAR}_i} - \overline{\beta_{\text{att.EAR}}})^2}}, \quad (6)$$

R shows the strength of a linear relationship between the CALIOP and EARLINET values. It ranges from -1 to $+1$, where a value of -1 means a total negative correlation, $+1$ is a total positive correlation and the value of 0 indicates no correlation.

The mean bias (MB) is defined as:

$$\text{MB} = \frac{1}{N} \sum_{i=1}^N (\beta_{\text{att.CAL}_i} - \beta_{\text{att.EAR}_i}), \quad (7)$$

where N is the number of the data points in the height range where both CALIOP and EARLINET attenuated backscatter data are available.

The factor of exceedance (FoE) which is defined as:

$$\text{FoE} = \left[\frac{N(\beta_{\text{att.CAL}} > \beta_{\text{att.EARL}})}{N} - 0.5 \right], \quad (8)$$

where $N(\beta_{\text{att.CAL}} > \beta_{\text{att.EAR}})$ is the number of data points in which CALIOP backscatter coefficient measurements are higher than the coincident EARLINET observations. The FoE value can vary between -0.5 (all CALIOP values are underestimated) and $+0.5$ (all CALIOP values are overestimated).

Title Page

Abstract

Introduction

Conclusions

References

Tables

Figures

◀

▶

◀

▶

Back

Close

Full Screen / Esc

Printer-friendly Version

Interactive Discussion



3 Results

3.1 Case studies

Two particular cases of CALIOP overpasses were chosen to demonstrate the methodology described in Sect. 2 and to show CALIOP's capability to detect aerosol layers under different conditions. CALIOP overpasses close to the Barcelona and Granada EARLINET stations are used in this illustration. The first overpass represents one of the best agreements between CALIOP and EARLINET stations out of 48 overpasses; the second overpass is an example of a case with discrepancies between the measurements by the two instruments.

The first case study was carried out using a CALIOP overpass over the Barcelona EARLINET station and it is an example of good agreement between EARLINET and CALIOP measurements in the PBL. The CALIOP overpass map is presented in Fig. 1. The attenuated CALIOP and EARLINET backscatter coefficients vs. altitude are shown in the left panel of Fig. 2. The aerosol type flag was assigned by the CALIOP aerosol classification algorithm (Liu et al., 2009) and it is presented in each case by different coloured dots in Fig. 2. The attenuated backscatter profiles agree well in the FT, and the PBL top was adequately distinguished by CALIOP (Fig. 2). The results show that the correlation between the two profiles is strong, with a correlation coefficient of 0.96. The factor of exceedance equals 0.1, which shows an overestimation of 60 % of the CALIOP data points. For this case, the calculated mean bias value was $0.1 \text{ Mm}^{-1} \text{ sr}^{-1}$.

The second case study was carried out for a CALIOP overpass over the Granada EARLINET station (Fig. 3) and it represents a Saharan dust event, which stretched from the region of western North Africa over Gibraltar towards the southern part of Spain. The hybrid single particle Lagrangian integrated trajectory model (HYSPLIT) (Draxler and Rolph, 2013,) was used to analyse the origin of the air mass. The backward trajectory analysis confirms that the air mass came from Africa, the Sahara region. The results of the analysis are shown in Fig. 4. The attenuated backscatter vs. altitude is shown in the left panel of Fig. 5. A dust layer is detected between 4 and 6.5 km by both

CALIOP near-real-time backscatter products

T. Grigas et al.

Title Page

Abstract

Introduction

Conclusions

References

Tables

Figures



Back

Close

Full Screen / Esc

Printer-friendly Version

Interactive Discussion



lidars, however, the CALIOP profile differs from the EARLINET profile at the higher altitudes by an amount outside the uncertainty bounds of the instruments. There are some additional discrepancies between CALIOP and EARLINET measurements (left panel of Fig. 5). The top of the CALIOP-detected dust layer is approximately 500 m higher.

There were two distinguishable aerosol layers in the EARLINET backscatter profile, namely the primary one between 5 and 6 km altitude and a secondary one around 2 km altitude. However, the secondary layer in the PBL region is barely distinguishable in the CALIOP profile.

Those differences between the two profiles could happen for two reasons. First, the measurements were performed at a separation distance of 67 km, and therefore CALIOP and EARLINET are not measuring exactly the same portion of the dust layer. Second, the CALIOP measurements were performed in the top down direction and there may be sufficient attenuation to make it more difficult to detect a second layer below. These issues influenced the mean bias and the correlation between backscatter profiles. As a result, the correlation between the two profiles is not as strong as in the first case: the correlation coefficient for this case was 0.47 while the mean bias was $-0.09 \text{ Mm}^{-1} \text{ sr}^{-1}$. Consequently, the factor of exceedance was -0.15 , which shows that 65 % of the CALIOP total attenuated backscatter values were lower than EARLINET values.

The next section provides an overview of the agreement between CALIOP and EARLINET attenuated backscatter values for all of the CALIOP overpasses with ground track offset distances of 100 km or less.

3.2 Summary of CALIOP overpasses with ground track distance ≤ 100 km

From November 2010 to December 2012, 48 CALIOP overpasses occurred within a 100 km distance from an operating EARLINET station, with aerosol layers classified as dust, polluted dust, clean marine, clean continental, polluted continental, mixed and/or smoke/biomass burning. These 48 overpasses resulted in 7405 data points that

were deemed valid for evaluation against EARLINET. The scatterplot of CALIOP and EARLINET attenuated backscatter values for all of these data points is shown in Fig. 6.

The CALIOP and EARLINET data correlate well ($R = 0.86$), with a mean bias equal to $0.03 \text{ Mm}^{-1} \text{ sr}^{-1}$, while the factor of exceedance value is 0.17. The latter statistical parameter indicates that 67 % of the CALIOP attenuated backscatter values were higher than the corresponding EARLINET measurements. However, there were several points that deviated from the 1 : 1 line. In order to investigate the cause of these outliers, the data were colour coded by the overpass distance (Fig. 6) and the vertical height of the aerosol layer (Fig. 7), which revealed that the majority of the outliers were observed when the distance between the EARLINET station and CALIPSO overpass exceeded 30 km. Moreover, the correlation seemed to be dependent on the height of the aerosol layer and on the presence of multiple layers in the FT and the PBL at the same time (as in the second case study). Therefore, further analysis was performed for the PBL and the FT separately.

3.3 PBL and FT with ground track distance ≤ 100 km

The PBL height was assumed to always be 2.5 km for this analysis (Mattis et al., 2004; Pappalardo et al., 2004). The scatterplots for the separated PBL and FT datasets are shown in Figs. 8 and 9. In our analysis, averaging of CALIOP data is performed along the closest 100 km ground tracks and the statistical agreement is characterized by R , MB and FoE parameters (Table 2).

The correlation is significantly stronger for the FT ($R = 0.85$) compared to the PBL ($R = 0.60$). The factor of exceedance for the FT equals 0.22, which indicates that 72 % of the CALIOP total attenuated backscatter values were higher than the EARLINET values, with a mean bias of $0.06 \text{ Mm}^{-1} \text{ sr}^{-1}$. Correspondingly, the FoE for the PBL was equal to -0.12 and MB = $-0.14 \text{ Mm}^{-1} \text{ sr}^{-1}$, which suggests that only 38 % of CALIOP values were higher than EARLINET values in the PBL.

Free tropospheric aerosol layers are more uniform and have less spatial variation, therefore the comparisons between CALIOP and EARLINET in the FT show higher

Title Page

Abstract

Introduction

Conclusions

References

Tables

Figures



Back

Close

Full Screen / Esc

Printer-friendly Version

Interactive Discussion



5 correlations. Boundary layer aerosol, on the other hand, is less homogeneous. That could be a result of the presence of aerosol layers in the FT and PBL at the same time. In this case, the first layer would attenuate the lidar signal and the signal would have less power to penetrate a second layer. To investigate that idea, data filtering with threshold values from the second case study were used. However, this choice reduced the amount of CALIOP overpasses from 48 down to 27, while the number of data points available for the comparison dropped from 7405 down to 3398.

3.4 PBL and FT using data filtering

10 In this analysis, the data points were selected from the CALIOP overpasses based on threshold values of the column backscatter coefficient (vertically summed values). These values were derived from the second case study (with aerosol layers present in both the PBL and FT) in two chosen altitudes ranges (up to 3 and above 3 km). The threshold column backscatter value for the altitude range up to 3 km was $38 \text{ M m}^{-1} \text{ sr}^{-1}$, while the value above 3 km was $71 \text{ M m}^{-1} \text{ sr}^{-1}$. Next, only CALIOP overpasses with detected aerosol with lower than these threshold values were used in the analysis. After applying such filtering, the statistics are presented in Table 3.

15 The scatterplots of the attenuated backscatter for CALIOP and EARLINET after applying this data filtering are presented in Figs. 10 and 11. The correlation between the two sets of attenuated backscatter measurements became stronger in the PBL ($R = 0.65$), while the same parameter for the FT decreased from $R = 0.85$ to $R = 0.79$. Correspondingly, the other statistical parameters improved for the PBL ($\text{MB} = -0.09$ and $\text{FoE} = -0.09$) and they decreased by a factor of two for the FT ($\text{MB} = 0.03$ and $\text{FoE} = 0.11$).

25 Filtering also improved the agreement between CALIOP and EARLINET for different types of aerosol in the PBL. Figures 12a and 13a show that clean air (according to the CALIOP documentation, this type is flagged when no aerosol is detected) cases have the best correlation (0.61 and 0.80, PBL and FT respectively) among all aerosol types, because clean air has very little spatial variability.

The clean marine type of aerosol was detected by CALIOP exclusively in the PBL (Fig. 12b), which is consistent with the marine surface source. However, a negative correlation coefficient was found for this aerosol type. One data point looks like an outlier. If this data point is removed, the statistics for clean marine aerosol type become the following: $R = 0.96$, $MB = 0$, $FoE = 0.01$.

The dust aerosol is usually transported over long distances in the FT (Fig. 13b), where its correlation is stronger ($R = 0.57$) compared to the PBL ($R = 0.46$, Fig. 12c), because the PBL aerosol is more affected by local sources.

The polluted dust aerosol detected by CALIOP represents a mix of dust and biomass burning/smoke aerosol. Both types of aerosol contribute to trans-boundary air pollution and are transported in the FT. However, the correlation coefficient for polluted dust aerosol is higher in the PBL ($R = 0.44$) than in the FT ($R = 0.38$) (Figs. 12d and 13c).

On the other hand, the polluted continental aerosol originates from local sources, which is consistent with the fact that CALIOP detected this type exclusively in the PBL (Fig. 12e); however, this localization affected CALIOP's ability to represent the variations of the polluted aerosol, because significant spatial averaging is required to obtain adequate SNR. Strong local sources could result in a very inhomogeneous aerosol distribution in the PBL, therefore, a poorer correlation ($R = 0.37$) between CALIOP and EARLINET could be a result of different area coverage for the two methods.

The mixed aerosol (Fig. 13d) was detected only in FT cases, with the lowest $R = 0.35$ value across all aerosol types. The reason for this is that it is a mix of other aerosol types, which causes a low value of the correlation coefficient.

4 Conclusions

Over three years, 48 CALIOP overpasses occurred within a 100 km ground track off-set distance from an operating EARLINET station, resulting in 7405 data points for the analysis presented here. The inter-comparison of the total attenuated backscatter profiles from near-real-time CALIOP Level 1.5 data and converted EARLINET

Title Page

Abstract

Introduction

Conclusions

References

Tables

Figures



Back

Close

Full Screen / Esc

Printer-friendly Version

Interactive Discussion



data showed fairly good agreement, with the correlation around 0.86, a mean bias of $0.03 \text{ M m}^{-1} \text{ sr}^{-1}$ and a factor of exceedance of 0.17. On average, the CALIOP attenuated backscatter values were slightly higher (by 3%) than the EARLINET values.

The level of agreement between the CALIOP and EARLINET attenuated backscatter values was influenced by the presence of aerosol layers in the PBL and FT and by the aerosol layer height. A type of data filtering was used to mitigate the multiple layers influence, and the filtering improved the agreement between the two data sets in the PBL. In addition, splitting the aerosol layer heights into two categories distinguished the differences between the PBL and the FT. Before applying the filtering, the CALIOP attenuated backscatter values were lower by 20% in the PBL compared to the EARLINET measurements, however, they were higher by 8% in the FT. After applying the filtering, the correlation coefficient improved (from $R = 0.60$ up to $R = 0.65$) within the PBL, and the mean bias decreased from $\text{MB} = -0.14 \text{ M m}^{-1} \text{ sr}^{-1}$ down to $\text{MB} = -0.09 \text{ M m}^{-1} \text{ sr}^{-1}$. The factor of exceedance decreased as well, from $\text{FoE} = -0.12$ to $\text{FoE} = -0.09$. Finally, the majority of the outliers in the regression plot of CALIOP and EARLINET attenuated backscatter were shown to be caused by the presence of layers in both the PBL and the FT.

The aerosol types detected by CALIOP were consistent with the source of the aerosol and the transport mechanism. Aerosols from local sources were mainly detected in the boundary layer, while long range transport pollution was observed in the FT. The correlation for different aerosol types was stronger within the FT and it was in the range of 0.35 to 0.80, with mean bias values of -0.24 to $0.27 \text{ M m}^{-1} \text{ sr}^{-1}$, and the factor of exceedance between -0.05 and 0.11. The correlation for the PBL was slightly weaker ($R = 0.37$ – 0.61) and the mean bias values were in the range of -0.19 to $0.19 \text{ M m}^{-1} \text{ sr}^{-1}$, with the factor of exceedance -0.16 to 0.02.

Acknowledgements. The authors gratefully acknowledge the European Union for funding this work under the 7 Framework Programme as the MACC-II subproject, and the Irish Research Council “New Foundations” programme. The authors acknowledge the CALIPSO scientific team for granting access to the CALIOP Level 1.5 data and EARLINET for providing aerosol

CALIOP
near-real-time
backscatter products

T. Grigas et al.

Title Page

Abstract

Introduction

Conclusions

References

Tables

Figures



Back

Close

Full Screen / Esc

Printer-friendly Version

Interactive Discussion



lidar profiles, which were available from the EARLINET webpage. The authors also acknowledge the NOAA Air Resources Laboratory (ARL) for the provision of the HYSPLIT transport and dispersion model used in this study.

References

- 5 Burton, S. P., Ferrare, R. A., Vaughan, M. A., Omar, A. H., Rogers, R. R., Hostetler, C. A., and Hair, J. W.: Aerosol classification from airborne HSRL and comparisons with the CALIPSO vertical feature mask, *Atmos. Meas. Tech.*, 6, 1397–1412, doi:10.5194/amt-6-1397-2013, 2013.
- 10 CALIPSO Quality Statements: CALIPSO Quality Statements Lidar Level 1.5 Data Product Version Release: 3.02, available at: https://eosweb.larc.nasa.gov/sites/default/files/project/calipso/quality_summaries/CAL_lidar_L1-5_v3-02.pdf (last access: 15 December 2014), 2011.
- 15 Draxler, R. R. and Rolph, G. D.: HYSPLIT (HYbrid Single-Particle Lagrangian Integrated Trajectory) Model access via NOAA ARL READY Website, available at: <http://www.arl.noaa.gov/HYSPLIT.php> (last access: 15 December 2014), 2013.
- Giannakaki, E., Balis, D. S., Amiridis, V., and Zerefos, C.: Optical properties of different aerosol types: seven years of combined Raman-elastic backscatter lidar measurements in Thessaloniki, Greece, *Atmos. Meas. Tech.*, 3, 569–578, doi:10.5194/amt-3-569-2010, 2010.
- 20 Groß, S., Gasteiger, J., Freudenthaler, V., Schnell, F., and Wiegner, M.: Characterization of the Eyjafjallajökull ash-plume by means of lidar measurements over the Munich EARLINET-site, *Proc. SPIE*, 7832, 78320M–78320M–8, 2010.
- Haywood, J., Francis, P., Dubovik, O., Glew, M., and Holben, B.: Comparison of aerosol size distributions, radiative properties, and optical depths determined by aircraft observations and Sun photometers during SAFARI 2000, *J. Geophys. Res.-Atmos.*, 108, 8471, doi:10.1029/2002JD002250, 2003.
- 25 Kristiansen, N. I., Stohl, A., Prata, A. J., Bukowiecki, N., Dacre, H., Eckhardt, S., Henne, S., Hort, M. C., Johnson, B. T., Marengo, F., Neiningner, B., Reitebuch, O., Seibert, P., Thomson, D. J., Webster, H. N., and Weinzierl, B.: Performance assessment of a volcanic ash transport model mini-ensemble used for inverse modeling of the 2010 Eyjafjallajökull

CALIOP
near-real-time
backscatter products

T. Grigas et al.

Title Page

Abstract

Introduction

Conclusions

References

Tables

Figures



Back

Close

Full Screen / Esc

Printer-friendly Version

Interactive Discussion



**CALIOP
near-real-time
backscatter products**

T. Grigas et al.

[Title Page](#)[Abstract](#)[Introduction](#)[Conclusions](#)[References](#)[Tables](#)[Figures](#)[Back](#)[Close](#)[Full Screen / Esc](#)[Printer-friendly Version](#)[Interactive Discussion](#)

eruption: Eyjafjallajökull ash transport modeling, *J. Geophys. Res.-Atmos.*, 117, D00U11, doi:10.1029/2011JD016844, 2012.

Liu, Z., Vaughan, M., Winker, D., Kittaka, C., Getzewich, B., Kuehn, R., Omar, A., Powell, K., Trepte, C., and Hostetler, C.: The CALIPSO lidar cloud and aerosol discrimination: version 2 algorithm and initial assessment of performance, *J. Atmos. Ocean. Tech.*, 26, 1198–1213, doi:10.1175/2009JTECHA1229.1, 2009.

Mamouri, R. E., Amiridis, V., Papayannis, A., Giannakaki, E., Tsaknakis, G., and Balis, D. S.: Validation of CALIPSO space-borne-derived attenuated backscatter coefficient profiles using a ground-based lidar in Athens, Greece, *Atmos. Meas. Tech.*, 2, 513–522, doi:10.5194/amt-2-513-2009, 2009.

Mattis, I., Ansmann, A., Müller, D., Wandinger, U., and Althausen, D.: Multiyear aerosol observations with dual-wavelength Raman lidar in the framework of EARLINET, *J. Geophys. Res.-Atmos.*, 109, D13203, doi:10.1029/2004JD004600, 2004.

Mattis, I., Mona, L., Müller, D., Pappalardo, G., Arboledas, L. A., Da'Mico, G., Amodeo, A., Apituley, A., Baldasano, J. M., Böckmann, C., Bösenberg, J., Chaikovskiy, A., Comeron, A., Giannakaki, E., Grigorov, I., Rascado, J. L. G., Gustafsson, O., Iarlori, M., Linné, H., Mitev, V., Francisco Molero Menéndez, D. N., Nicolae, D., Papayannis, A., García-Pando, C. P., Perrone, M. R., Pietruczuk, A., Putaud, J.-P., Ravetta, F., Rodríguez, A., Seifert, P., Sicard, M., Simeonov, V., Sobolewski, P., Spinelli, N., Stebel, K., Stohl, A., Tesche, M., Trickl, T., Wang, X., and Wiegner, M.: EARLINET correlative measurements for CALIPSO, in: *Proceedings of SPIE – The International Society for Optical Engineering*, Vol. 6750, doi:10.1117/12.738090, 2007.

Mattis, I., Müller, D., Ansmann, A., Wandinger, U., Preißler, J., Seifert, P., and Tesche, M.: Ten years of multiwavelength Raman lidar observations of free-tropospheric aerosol layers over central Europe: geometrical properties and annual cycle, *J. Geophys. Res.-Atmos.*, 113, D20202, doi:10.1029/2007JD009636, 2008.

Molero, F. and Pujadas, M.: Comparison of correlative measurements of CALIPSO lidar and the #21 EARLINET station (CIEMAT-Madrid), in: *Proceedings of SPIE – The International Society for Optical Engineering*, Vol. 7111, doi:10.1117/12.799745, 2008.

Mona, L., Pappalardo, G., Amodeo, A., D'Amico, G., Madonna, F., Boselli, A., Giunta, A., Russo, F., and Cuomo, V.: One year of CNR-IMAA multi-wavelength Raman lidar measurements in coincidence with CALIPSO overpasses: Level 1 products comparison, *Atmos. Chem. Phys.*, 9, 7213–7228, doi:10.5194/acp-9-7213-2009, 2009.

CALIOP near-real-time backscatter products

T. Grigas et al.

Title Page

Abstract

Introduction

Conclusions

References

Tables

Figures



Back

Close

Full Screen / Esc

Printer-friendly Version

Interactive Discussion



Omar, A. H., Winker, D. M., Vaughan, M. A., Hu, Y., Treppe, C. R., Ferrare, R. A., Lee, K.-P., Hostetler, C. A., Kittaka, C., Rogers, R. R., Kuehn, R. E., and Liu, Z.: The CALIPSO automated aerosol classification and lidar ratio selection algorithm, *J. Atmos. Ocean. Tech.*, 26, 1994–2014, doi:10.1175/2009JTECHA1231.1, 2009.

5 Papayannis, A., Chourdakis, G., Tsaknakis, G., and Serafetinides, A.: One-year observations of the vertical structure of Saharan dust over Athens, Greece monitored by NTUA's lidar system in the frame of EARLINET, in: *Proceedings of SPIE – The International Society for Optical Engineering*, Vol. 4539, 146–157, doi:10.1117/12.454434, 2002.

10 Pappalardo, G., Amodeo, A., Mona, L., Pandolfi, M., Pergola, N., and Cuomo, V.: Raman lidar observations of aerosol emitted during the 2002 Etna eruption, *Geophys. Res. Lett.*, 31, L05120, doi:10.1029/2003GL019073, 2004.

15 Pappalardo, G., Mona, L., Wandinger, U., Mattis, I., Amodeo, A., Ansmann, A., Apituley, A., Alados-Arboledas, L., Balis, D., Chaikovskiy, A., Comeron, A., D'Amico, G., Freudenthaler, V., Giunta, A., Grigorov, I., Hiebsch, A., Linné, H., Madonna, F., Papayannis, A., Perrone, M. R., Pietruczuk, A., Pujadas, M., Rizi, V., Spinelli, N., and Wiegner, M.: Analysis of the EARLINET correlative measurements for CALIPSO, *Proc. SPIE*, 7479, 74790B–74790B, doi:10.1117/12.830323, 2009a.

20 Pappalardo, G., Mona, L., Wandinger, U., Mattis, I., Amodeo, A., Ansmann, A., Apituley, A., Arboledas, L. A., Balis, D., Chaikovskiy, A., Comeron, A., D'Amico, G., Freudenthaler, V., Giunta, A., Grigorov, I., Hiebsch, A., Linné, H., Madonna, F., Papayannis, A., Perrone, M. R., Pietruczuk, A., Pujadas, M., Rizi, V., Spinelli, N., and Wiegner, M.: Analysis of the EARLINET correlative measurements for CALIPSO, in: *Proceedings of SPIE – The International Society for Optical Engineering*, Vol. 7479, doi:10.1029/2009JD012147, 2009b.

25 Pappalardo, G., Wandinger, U., Mona, L., Hiebsch, A., Mattis, I., Amodeo, A., Ansmann, A., Seifert, P., Linné, H., Apituley, A., Alados Arboledas, L., Balis, D., Chaikovskiy, A., D'Amico, G., De Tomasi, F., Freudenthaler, V., Giannakaki, E., Giunta, A., Grigorov, I., Iarlori, M., Madonna, F., Mamouri, R.-E., Nasti, L., Papayannis, A., Pietruczuk, A., Pujadas, M., Rizi, V., Rocadenbosch, F., Russo, F., Schnell, F., Spinelli, N., Wang, X., and Wiegner, M.: EARLINET correlative measurements for CALIPSO: first intercomparison results, *J. Geophys. Res.-Atmos.*, 115, D00H19, doi:10.1029/2009JD012147, 2010.

30 Powell, K., Vaughan, M., Winker, D., Lee, K.-P., Pitts, M., Treppe, C., Detweiler, P., Hunt, W., Lambeth, J., Lucker, P., Murray, T., Hagolle, O., Lifermann, A., Faivre, M., Garnier, A., and Pelon, J.: Cloud – Aerosol LIDAR Infrared Pathfinder Satellite Observations (CALIPSO), *Data Man-*

agement System, Data Products Catalog, Document No: PC-SCI-503, Release 3.2, August 2010, NASA Langley Research Center, Hampton, Virginia, USA, 2010.

Rolph, G. D.: Real-time Environmental Applications and Display System (READY) Website, available at: <http://www.ready.noaa.gov> (last access: 15 December 2014), 2013.

5 Sawamura, P., Vernier, J., Barnes, J., Berkoff, T., Welton, E., Alados-Arboledas, L., Navas-Guzmán, F., Pappalardo, G., Mona, L., Madonna, F., Lange, D., Sicard, M., Godin-Beekmann, S., Payen, G., Wang, Z., Hu, S., Tripathi, S., Cordoba-Jabonero, C., and Hoff, R.: Stratospheric AOD after the 2011 eruption of Nabro volcano measured by lidars over the Northern Hemisphere, *Environ. Res. Lett.*, 7, 034013, doi:10.1088/1748-9326/7/3/034013, 2012.

10 Sekiyama, T. T., Tanaka, T. Y., Shimizu, A., and Miyoshi, T.: Data assimilation of CALIPSO aerosol observations, *Atmos. Chem. Phys.*, 10, 39–49, doi:10.5194/acp-10-39-2010, 2010.

Stephens, G. L., Vane, D. G., Boain, R. J., Mace, G. G., Sassen, K., Wang, Z., Illingworth, A. J., O'Connor, E. J., Rossow, W. B., Durden, S. L., Miller, S. D., Austin, R. T., Benedetti, A., and Mitrescu, C.: The cloudsat mission and the A-Train: a new dimension of space-based observations of clouds and precipitation, *B. Am. Meteorol. Soc.*, 83, 1771–1790 + 1742, 2002.

15 Wang, Y., Sartelet, K. N., Bocquet, M., and Chazette, P.: Assimilation of ground versus lidar observations for PM₁₀ forecasting, *Atmos. Chem. Phys.*, 13, 269–283, doi:10.5194/acp-13-269-2013, 2013.

20 Winker, D. M., Vaughan, M. A., Omar, A., Hu, Y., Powell, K. A., Liu, Z., Hunt, W. H., and Young, S. A.: Overview of the CALIPSO mission and CALIOP data processing algorithms, *J. Atmos. Ocean. Tech.*, 26, 2310–2323, doi:10.1175/2009JTECHA1281.1, 2009.

25 Yu, H., Kaufman, Y. J., Chin, M., Feingold, G., Remer, L. A., Anderson, T. L., Balkanski, Y., Belouin, N., Boucher, O., Christopher, S., DeCola, P., Kahn, R., Koch, D., Loeb, N., Reddy, M. S., Schulz, M., Takemura, T., and Zhou, M.: A review of measurement-based assessments of the aerosol direct radiative effect and forcing, *Atmos. Chem. Phys.*, 6, 613–666, doi:10.5194/acp-6-613-2006, 2006.

CALIOP
near-real-time
backscatter products

T. Grigas et al.

Title Page

Abstract

Introduction

Conclusions

References

Tables

Figures



Back

Close

Full Screen / Esc

Printer-friendly Version

Interactive Discussion



[Title Page](#)[Abstract](#)[Introduction](#)[Conclusions](#)[References](#)[Tables](#)[Figures](#)[Back](#)[Close](#)[Full Screen / Esc](#)[Printer-friendly Version](#)[Interactive Discussion](#)**Table 1.** EARLINET stations that had coincident measurements with CALIOP during the observational period.

Nr.	Station Code	Station name, location	Coordinates
1	at	Athens, Greece	37.96° N, 23.78° E
2	ba	Barcelona, Spain	41.389° N, 2.112° E
3	be	Belsk, Poland	51.84° N, 20.79° E
4	bu	Bucharest, Romania	44.348° N, 26.029° E
5	ca	Cabauw, Netherlands	51.97° N, 4.93° E
6	ev	Evora, Portugal	38.568° N, 7.912° W
7	gr	Granada, Spain	37.164° N, 3.605° W
8	hh	Hamburg, Germany	53.568° N, 9.973° E
9	is	Ispra, Italy	45.811° N, 8.621° E
10	ma	Madrid, Spain	40.456° N, 3.726° W
11	ms	Maisach, Germany	48.209° N, 11.258° E
12	na	Napoli, Italy	40.838° N, 14.183° E
13	pl	Palaiseau, France	48.7° N, 2.2° E
14	po	Potenza, Italy	40.601° N, 15.724° E

CALIOP
near-real-time
backscatter products

T. Grigas et al.

[Title Page](#)[Abstract](#)[Introduction](#)[Conclusions](#)[References](#)[Tables](#)[Figures](#)[Back](#)[Close](#)[Full Screen / Esc](#)[Printer-friendly Version](#)[Interactive Discussion](#)**Table 2.** Statistics of CALIOP and EARLINET agreement within the PBL and the FT with ground track distance within 100 km.

Region	<i>R</i>	MB ($\text{M m}^{-1} \text{sr}^{-1}$)	FoE
Entire range	0.86	0.03	0.17
PBL	0.60	−0.14	−0.12
FT	0.85	0.06	0.22

CALIOP near-real-time backscatter products

T. Grigas et al.

Title Page

Abstract

Introduction

Conclusions

References

Tables

Figures



Back

Close

Full Screen / Esc

Printer-friendly Version

Interactive Discussion



Table 3. Statistics of CALIOP and EARLINET agreement within the PBL and the FT using data filtering.

Region	R	MB ($\text{M m}^{-1} \text{sr}^{-1}$)	FoE
Entire range	0.84	0.01	0.08
PBL	0.65	-0.09	-0.09
FT	0.79	0.03	0.11

CALIOP
near-real-time
backscatter products

T. Grigas et al.

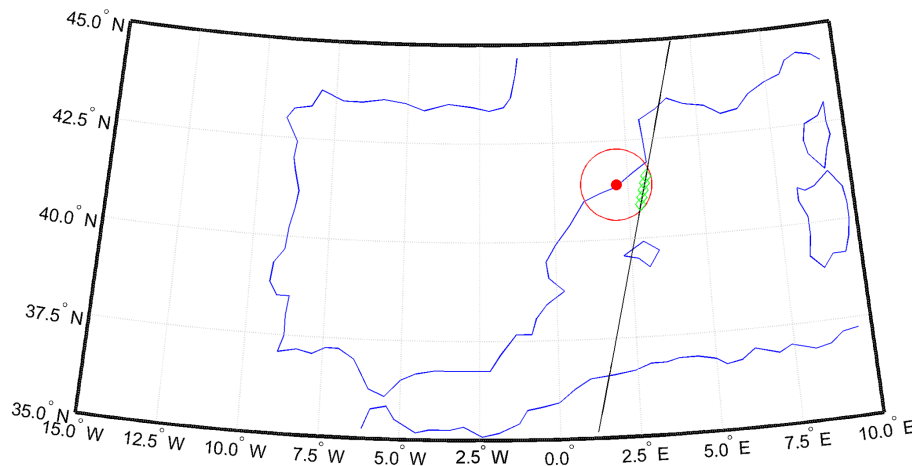


Figure 1. CALIOP overpass over Barcelona station on 20 September 2011 at 02:00 UTC at 77.9 km distance from the station. The red circle shows 100 km distance from the EARLINET station (the red dot in the center). The black line represents the CALIOP ground track, while the green empty diamonds represent five CALIOP profiles that were averaged and compared to EARLINET measurements.

[Title Page](#)[Abstract](#)[Introduction](#)[Conclusions](#)[References](#)[Tables](#)[Figures](#)[Back](#)[Close](#)[Full Screen / Esc](#)[Printer-friendly Version](#)[Interactive Discussion](#)

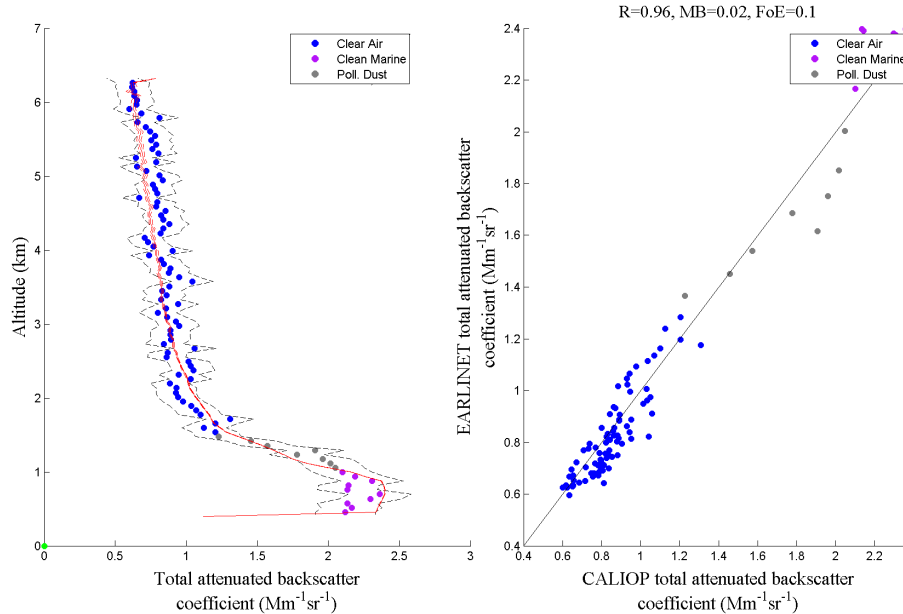


Figure 2. Left panel: Attenuated backscatter vs. altitude for a CALIOP overpass at Barcelona station on 20 September 2011 at 02:00 UTC at 77.9 km distance from the station, (the red line shows the EARLINET attenuated backscatter profile, the red dashed lines show EARLINET uncertainties, the dots represent CALIOP data, and the black dashed lines show the CALIOP uncertainties); right panel: corresponding scatterplot of CALIOP attenuated backscatter (different colours represents different detected aerosol type; see legend) against EARLINET attenuated backscatter with a 1 : 1 reference line (black).

**CALIOP
near-real-time
backscatter products**

T. Grigas et al.

Title Page	
Abstract	Introduction
Conclusions	References
Tables	Figures
◀	▶
◀	▶
Back	Close
Full Screen / Esc	
Printer-friendly Version	
Interactive Discussion	



CALIOP near-real-time backscatter products

T. Grigas et al.

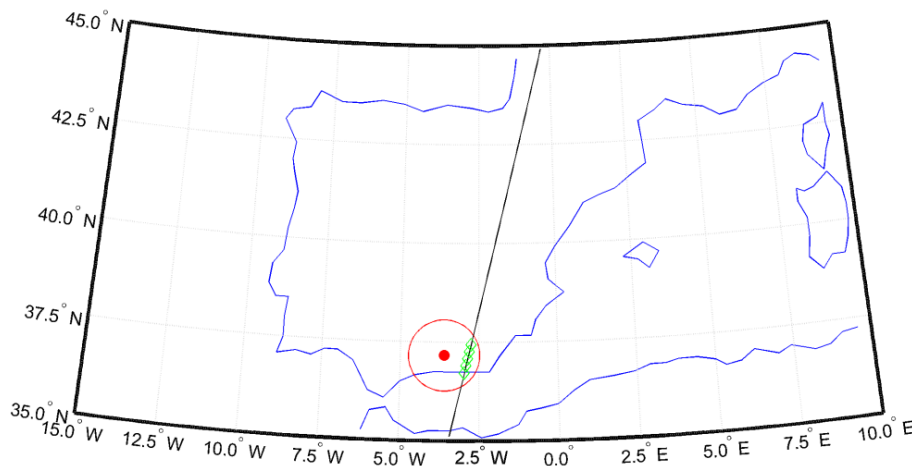


Figure 3. CALIOP overpass over Granada station on 7 July 2011 at 02:20 UTC at 67 km distance from the station. The red circle shows 100 km distance from EARLINET station (the red dot in the center). The black line represents the CALIOP ground track while the green empty diamonds represent five CALIOP profiles that were averaged and compared to EARLINET measurements.

[Title Page](#)[Abstract](#)[Introduction](#)[Conclusions](#)[References](#)[Tables](#)[Figures](#)[Back](#)[Close](#)[Full Screen / Esc](#)[Printer-friendly Version](#)[Interactive Discussion](#)

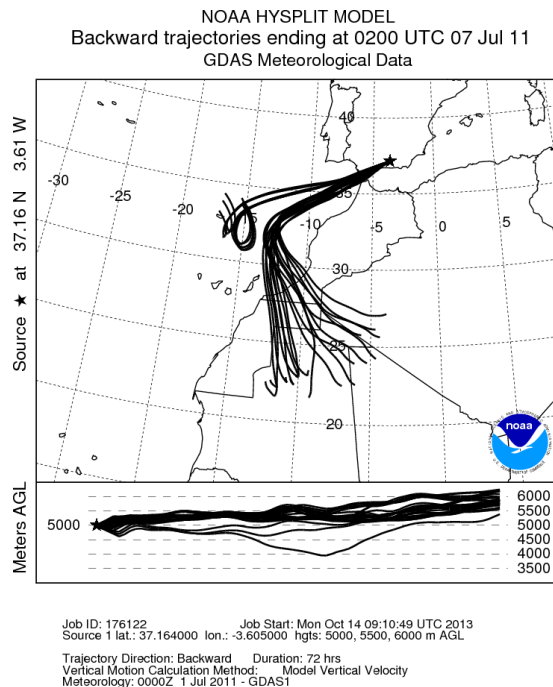


Figure 4. Hysplit backward trajectories for the overpass over the EARLINET station in Granada on 7 July 2011 at 02:00 UTC confirm that the air mass came from the region of western North Africa, over Gibraltar, and towards the southern part of Spain.

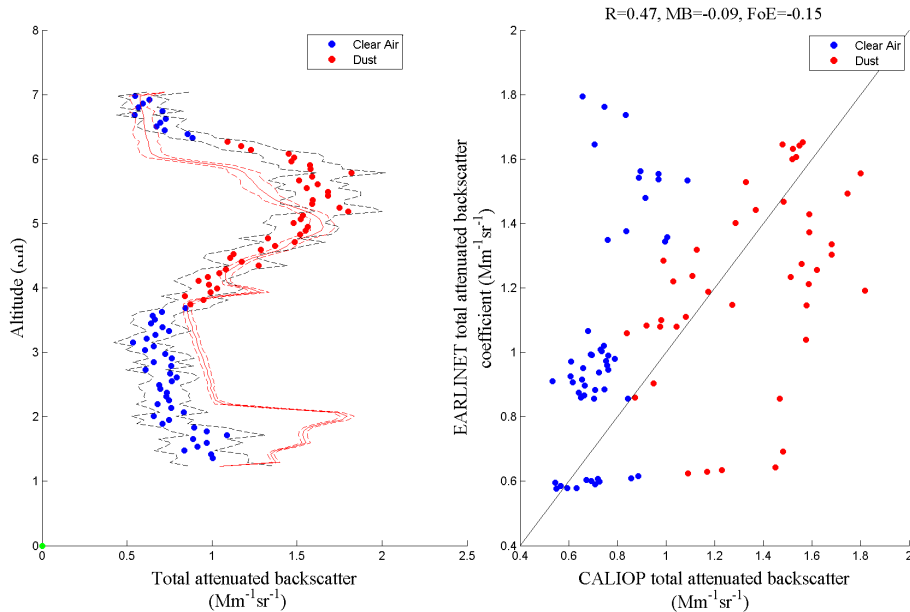


Figure 5. Left panel: Attenuated backscatter vs. altitude for a CALIOP overpass over Granada station on 7 July 2011 at 02:20 UTC at 67 km distance from the station (the red line shows the EARLINET attenuated backscatter profile, the red dashed lines show EARLINET uncertainties, the dots represent CALIOP data, and the dashed lines show the CALIOP uncertainty); right panel: corresponding scatterplot of CALIOP attenuated backscatter (different colours represents different detected aerosol; see legend) against EARLINET attenuated backscatter, with a 1 : 1 reference line (black).

CALIOP
near-real-time
backscatter products

T. Grigas et al.

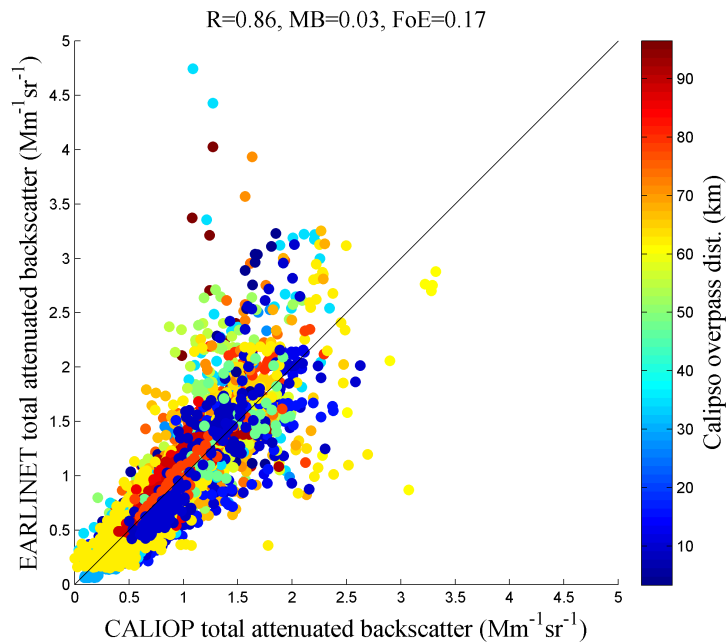


Figure 6. CALIOP vs. EARLINET total attenuated backscatter for CALIOP overpasses over EARLINET stations within 100 km ground track offset distance. The colour scale shows the ground track distance from the EARLINET station.

[Title Page](#)[Abstract](#)[Introduction](#)[Conclusions](#)[References](#)[Tables](#)[Figures](#)[Back](#)[Close](#)[Full Screen / Esc](#)[Printer-friendly Version](#)[Interactive Discussion](#)

CALIOP
near-real-time
backscatter products

T. Grigas et al.

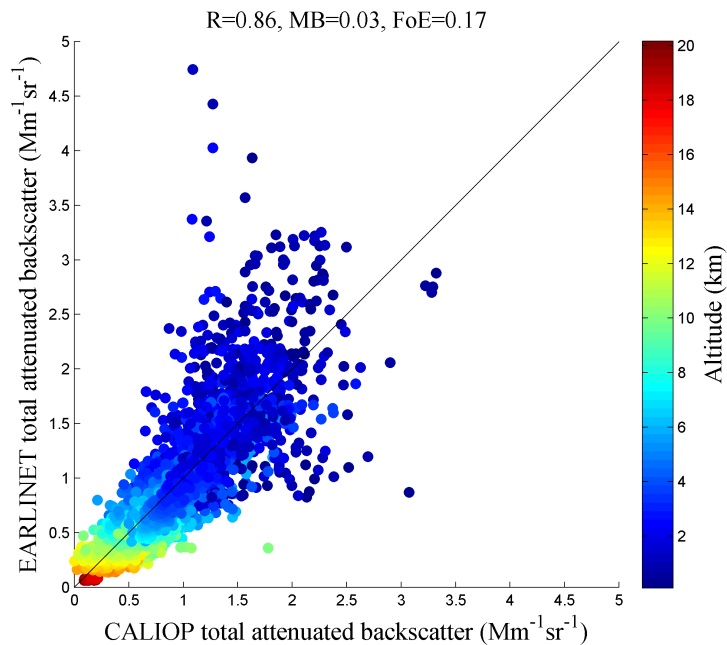


Figure 7. CALIOP vs. EARLINET total attenuated backscatter for CALIOP overpasses over EARLINET stations points within 100 km ground track distance, with colour coding showing the aerosol layer altitude.

[Title Page](#)[Abstract](#)[Introduction](#)[Conclusions](#)[References](#)[Tables](#)[Figures](#)[◀](#)[▶](#)[◀](#)[▶](#)[Back](#)[Close](#)[Full Screen / Esc](#)[Printer-friendly Version](#)[Interactive Discussion](#)

**CALIOP
near-real-time
backscatter products**

T. Grigas et al.

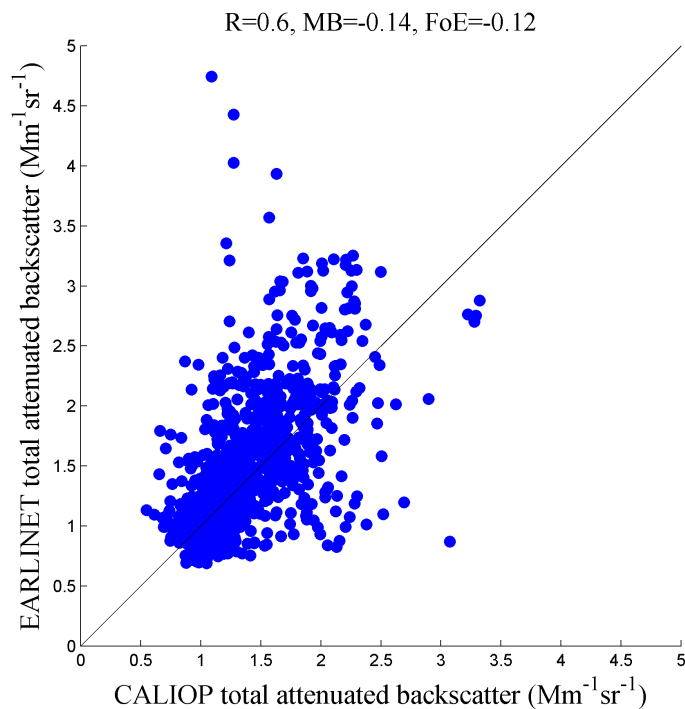


Figure 8. CALIOP vs. EARLINET total attenuated backscatter for CALIOP overpasses over EARLINET stations for the PBL only, within 100 km ground track distance.

Title Page

Abstract

Introduction

Conclusions

References

Tables

Figures



Back

Close

Full Screen / Esc

Printer-friendly Version

Interactive Discussion



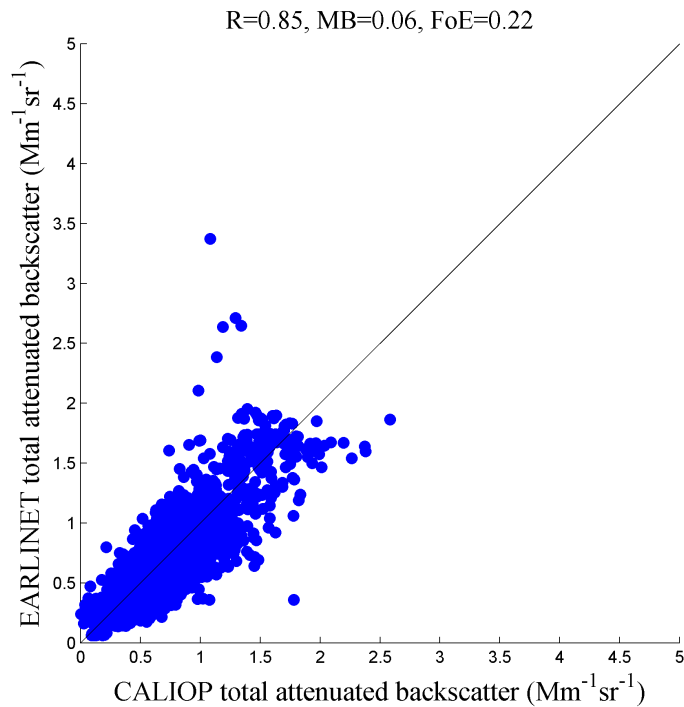


Figure 9. CALIOP vs. EARLINET total attenuated backscatter for CALIOP overpasses over EARLINET stations for the FT only, within 100 km ground track distance.

**CALIOP
near-real-time
backscatter products**

T. Grigas et al.

Title Page	
Abstract	Introduction
Conclusions	References
Tables	Figures
◀	▶
◀	▶
Back	Close
Full Screen / Esc	
Printer-friendly Version	
Interactive Discussion	



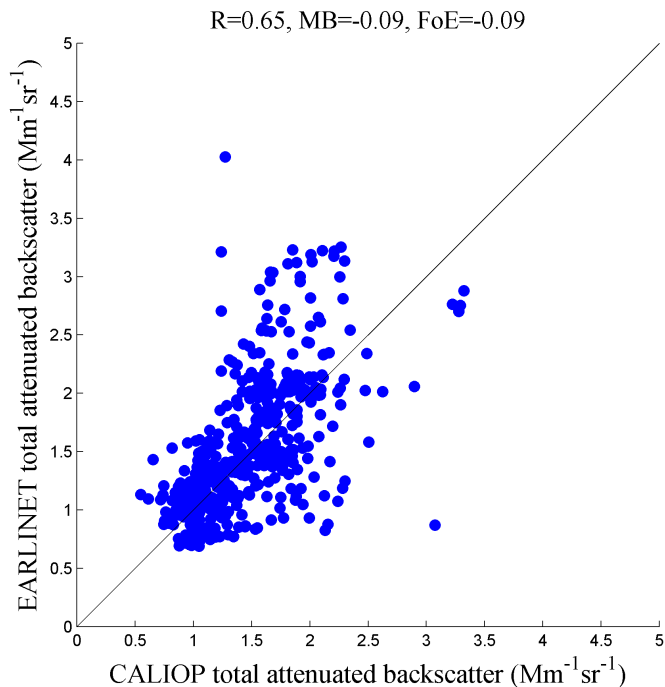


Figure 10. CALIOP vs. EARLINET total attenuated backscatter for CALIOP overpasses over EARLINET stations only for PBL. The plot includes all data points for overpasses without layers present in both the PBL and the FT.

**CALIOP
near-real-time
backscatter products**

T. Grigas et al.

Title Page

Abstract

Introduction

Conclusions

References

Tables

Figures

◀

▶

◀

▶

Back

Close

Full Screen / Esc

Printer-friendly Version

Interactive Discussion



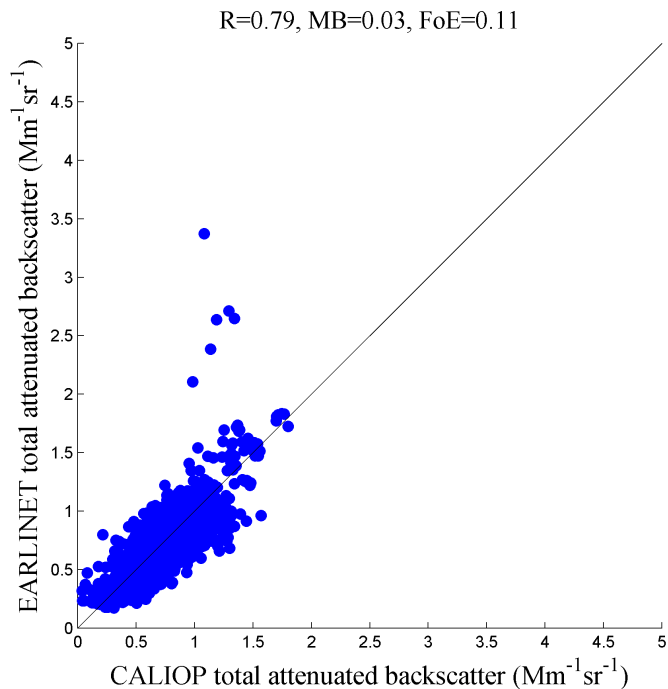


Figure 11. CALIOP vs. EARLINET total attenuated backscatter for CALIOP overpasses over EARLINET stations within 100 km overpass distance only for FT. The plot includes all data points for overpasses without present layers present in both the the PBL and the FT.

**CALIOP
near-real-time
backscatter products**

T. Grigas et al.

Title Page

Abstract

Introduction

Conclusions

References

Tables

Figures

◀

▶

◀

▶

Back

Close

Full Screen / Esc

Printer-friendly Version

Interactive Discussion



CALIOP near-real-time backscatter products

T. Grigas et al.

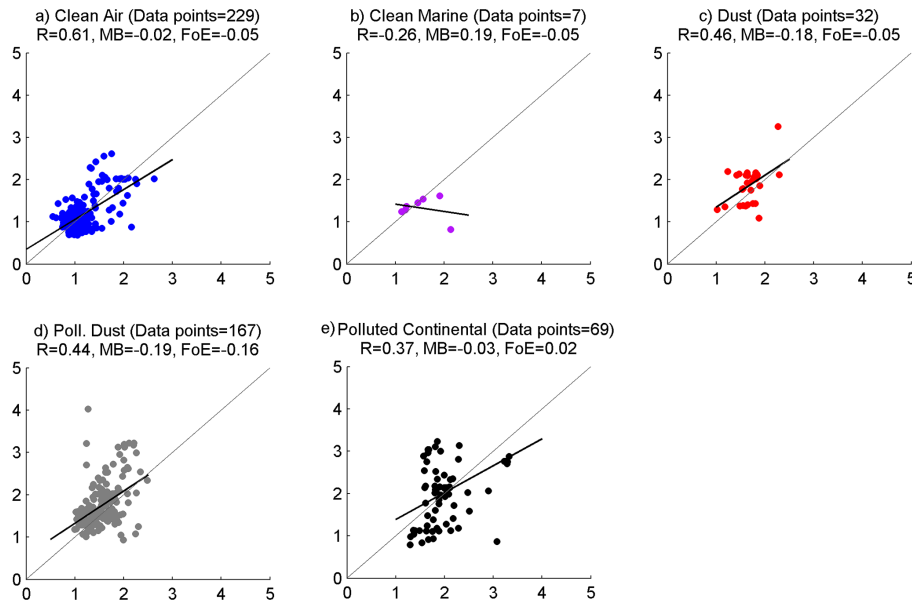


Figure 12. Eight aerosol types for CALIOP overpasses over EARLINET stations for the PBL. The plot includes filtered data points for overpasses without layers present in both the PBL and the FT.

Title Page

Abstract

Introduction

Conclusions

References

Tables

Figures

◀

▶

◀

▶

Back

Close

Full Screen / Esc

Printer-friendly Version

Interactive Discussion



CALIOP near-real-time backscatter products

T. Grigas et al.

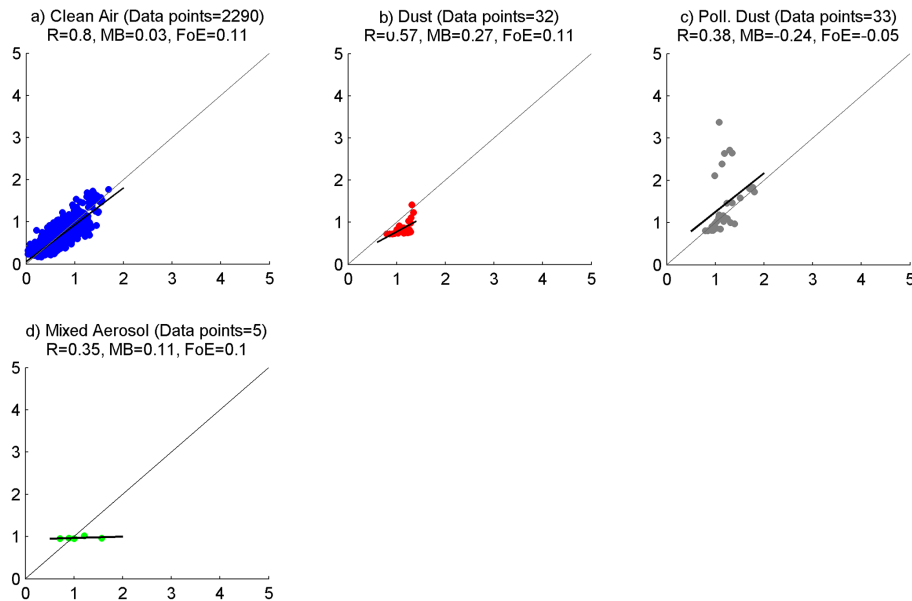


Figure 13. Eight aerosol types for CALIOP overpasses over EARLINET stations for the FT. The plot includes filtered data points for overpasses without layers present in both the PBL and the FT.

Title Page

Abstract

Introduction

Conclusions

References

Tables

Figures

◀

▶

◀

▶

Back

Close

Full Screen / Esc

Printer-friendly Version

Interactive Discussion

